ResearchGate

See discussions, stats, and author profiles for this publication at: https://www.researchgate.net/publication/359684218

Description of an Enigmatic Alveolate, Platyproteum noduliferae n. sp., and Reconstruction of its Flagellar Apparatus

Article *in* Protist · April 2022

DOI: 10.1016/j.protis.2022.125878

CITATIONS
0

READS
50

6 authors, including:

Koh Yokouchi
Hokkaido University
5 PUBLICATIONS **13** CITATIONS

SEE PROFILE

Davis Iritani
Agriculture and Agri-Food Canada
11 PUBLICATIONS **46** CITATIONS

SEE PROFILE

Kevin Wakeman
Hokkaido University
68 PUBLICATIONS **308** CITATIONS

SEE PROFILE

Some of the authors of this publication are also working on these related projects:

Microturbellarians of British Columbia View project

Sea Around Us View project

All content following this page was uploaded by Kevin Wakeman on 22 April 2022.

The user has requested enhancement of the downloaded file.

Protist 173 (2022) 125878
http://www.elsevier.de/protis
Published online date

Protist

ORIGINAL PAPER

Description of an Enigmatic Alveolate, *Platyproteum noduliferae* n. sp., and Reconstruction of its Flagellar Apparatus

Koh Yokouchi [a], Davis Iritani [a], Kay Hian Lim [b], Yong Heng Phua [b], Takeo Horiguchi [c], and Kevin C. Wakeman [d,1]

[a]Department of Natural History Sciences, Graduate School of Science, Hokkaido University, 060-0810 Sapporo, Japan
[b]School of Science, Hokkaido University, North 10, West 8, Sapporo 060-0810, Japan
[c]Department of Biological Sciences, Faculty of Science, Hokkaido University, 060-0817 Sapporo, Japan
[d]Institute for the Advancement of Higher Education, Hokkaido University, 060-0810 Sapporo, Japan

Submitted October 14, 2021; Accepted March 27, 2022
Monitoring Editor: Mona Hoppenrath

Platyproteum **is an enigmatic, monotypic genus formerly assigned to the Apicomplexa, until a recent phylogenomic study demonstrated that it diverged from the base of the chromerid/colpodellid (chrompodellid) taxa and apicomplexan clade. In the present study, a new species, *P. noduliferae* n. sp., is described using a combination of morphological and molecular data. Moreover, a reconstruction of the flagellar apparatus is presented to characterize the presence of flagella which was, until this study, an unknown trait for this genus. Phylogenetic analyses using rDNA sequences suggested that *P. noduliferae* n. sp. is a sister species of *P. vivax*, diverging from the base of chrompodellids and apicomplexans. This study provides new morphological data that corroborates the position of *Platyproteum* amongst other biflagellate species, contributing to an improved understanding of *Platyproteum* and the evolutionary changes undergone by some marine alveolates as they transitioned into obligate parasitic life styles.**
© 2022 Elsevier GmbH. All rights reserved.

Key words: Alveolate; evolutionary morphology; flagellar apparatus; marine parasites; systematics; ultrastructure.

Introduction

Apicomplexans, dinoflagellates and their relatives fall under a group known as the Myzozoa (Cavalier-Smith and Chao, 2004). Apicomplexa are obligate parasites of numerous animal hosts with over 6000 named species classified in 350 genera (Adl et al. 2019). Included in this group are

[1] Corresponding author; fax +81 11 706 4851
e-mail: wakeman.k@oia.hokudai.ac.jp (K.C. Wakeman).

https://doi.org/10.1016/j.protis.2022.125878
1434-4610/© 2022 Elsevier GmbH. All rights reserved.

infamous taxa such as *Plasmodium*, *Toxoplasma* and *Cryptosporidium* that have attracted special attention due to their medical or veterinary significance. Dinoflagellates also represent a major myzozoan lineage with species classified in over 300 genera including Perkinsozoa, *Oxyrrhis*, Syndiniales and 'core' dinoflagellates that employ various life style strategies including autotrophy, heterotrophy and parasitism (Adl et al., 2019; Hoppenrath, 2017; Janouškovec et al., 2017). Many other myzozoans, including chromerids and colpodellids, form a sister group to Apicomplexa, collectively referred to as chrompodellids (Janouškovec et al., 2015; Mathur et al., 2019). The discovery and understanding of these more enigmatic myzozoan lineages that have either retained ancestral characteristics or have been highly modified (e.g., to live as symbionts/parasites) has greatly improved our view of the evolutionary history of myzozoans (Cavalier-Smith, 2004; Janouškovec et al., 2015; Kuvardina et al., 2002). Specifically, dinoflagellates and chrompodellids are characteristically biflagellate, while flagella/cilia are generally limited to the male microgametes of certain apicomplexan taxa (Adl et al., 2019; Cavalier-Smith, 2004; Moore et al., 2008; Simpson and Patterson, 1996). This suggests that despite the parasitic nature of extant apicomplexans, the ancestor of the group was a free-living, biflagellate organism (Cavalier-Smith, 2004; Leander, 2008; Leander and Keeling, 2003). This evolutionary transition to parasitism has been a topic of great interest. Cytoskeletal components such as the flagellar apparatus have been studied in dinoflagellates and chrompodellids as informative traits for understanding myzozoan evolution (Francia and Striepen, 2014; Leander and Keeling, 2003; Okamoto and Keeling, 2014; Portman et al., 2014). Further species identification and morphological characterization are necessary to gain an accurate view of myzozoan evolutionary history which is hindered greatly by limited taxon sampling (Morrison, 2009).

Platyproteum is a genus of single-celled parasites found in the intestinal tract of sipunculid (peanut worm) hosts (Gunderson and Small, 1986; Leander, 2006; Leander and Keeling, 2003; Rueckert and Leander, 2009). The type species for the genus, *Platyproteum vivax* (ex. *Selenidium vivax*), was discovered in the host *Phascolosoma agassizii* (Gunderson and Small, 1986). This first report of *P. vivax* emphasized morphological observation and classified the new species into an existing genus of marine gregarine apicomplexans, *Selenidium*, while noting that there were morphological differences between its congeners in terms of size, plasticity in cell shape and the lack of permanent superficial striations at the light microscope level (Gunderson and Small, 1986). The authors also noted a "small, refractile body" that was visible at the tip of living cells, but not in stained specimens. A subsequent ultrastructural analysis was conducted that observed both internal and external morphology in great detail (Leander, 2006; Leander and Keeling, 2003). Interestingly, the presence of pores and vermiform structures protruding from these pores were noted in these ultrastructural observations. The SSU rDNA for *P. vivax* was sequenced by Rueckert and Leander (2009) and molecular phylogenetic analysis suggested that *P. vivax* should be removed from *Selenidium*. *Platyproteum* was proposed as a new genus to accommodate this taxonomic change. Most recently, a phylogenomic analysis incorporating several new transcriptomes, including a *Platyproteum* sp., showed that *Platyproteum* falls outside of the apicomplexan clade, and is instead an early-diverging myzozoan lineage (Mathur et al., 2019).

In the present study, we characterize an undescribed species of *Platyproteum*, *P. noduliferae* n. sp., discovered in the host *Phascolosoma noduliferum* Stimpson, 1855 on the western coast of Hokkaido, Japan. Morphological features, including the presence of flagella in the adult stages, are shown using light, scanning electron and transmission electron microscopy. Serial sections of the flagellar apparatus and a schematic reconstruction are also presented. Finally, a molecular phylogenetic analysis of rDNA sequences shows that *P. noduliferae* n. sp. is sister to *P. vivax*, branching from the base of chrompodellids and apicomplexans. The discovery and characterization of these early myzozoan lineages are crucial to informing the evolutionary history of alveolate parasitism. This study contributes to that effort by presenting the first characterization of the flagellar apparatus in this enigmatic genus.

Results

Morphology and Flagellar Apparatus

Trophozoites were prevalent in 100% of sampled hosts. They were flattened with a dynamically changing profile. Trophozoites were roughly elliptic with a general shape resembling that of a crescent

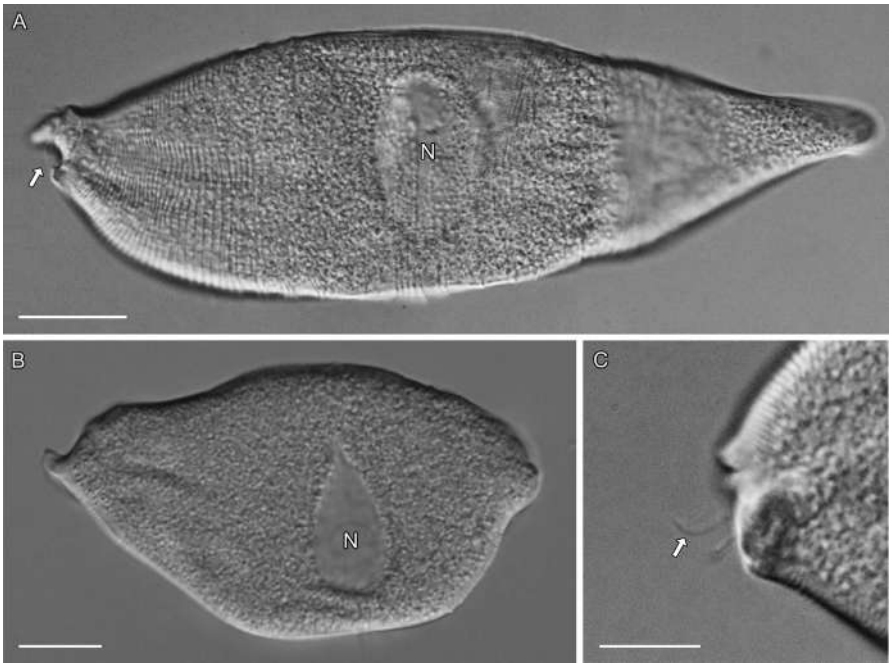

Figure 1. Light micrographs of living cells of *Platyproteum noduliferae* n. sp. taken in differential interference contrast (DIC) microscopy, showing trophozoite morphology. Mucron oriented to the left. (**A**) Stretched and (**B**) contracted cell. (**C**) Apical view of a cell. Note, oval nucleus (N) situated just posterior to the transverse midline of the cell. Two flagella protruding from the apical end of the cell (arrow). Scale bars: A, B = 20 μm; C = 10 μm.

or leaf (Fig. 1A). A typical trophozoite would be observed undergoing repeated cycles: starting from a flattened, leaf-like shape, stretching along the anteroposterior axis and creating a constriction near the middle of the cell body, followed by a steady contraction along the same axis to form a nearly spherical shape, then finally relaxing back to the initial flattened, leaf-like shape (Fig. 1A, B). Although the size of the trophozoite was never constant, it generally ranged between 111–121 lm in length and 29–43 lm in width (n = 40), while in its leaf-like shape. The nucleus was oval, measuring 16–17 lm along the major axis and 10–13 lm along the minor axis (n = 40), and situated just posterior to the transverse midline of the cell (Fig. 1A, B). A mucron at the anterior of the cell showed a hook-like shape (Fig. 1A, B). Short flagella were positioned in parallel at its anterior end (Fig. 1A, C) and could be seen beating in a whip-like motion (Supplementary Material Movie S1). The trophozoites showed a significant peristalsis-like movement (Fig. 2). No gliding motility or directional locomotion was observed.

SEM observation revealed numerous longitudinal striations running the surface of the whole cell (Fig. 3A). In addition, the apical part of the cell showed both longitudinal and transverse striations that formed a criss-cross lattice of 2 by 2 folds/lm (Fig. 3). The two flagella, which are termed as anterior flagellum (AF) and posterior flagellum (PF), protruded from the base of mucron at the apical end of cell (Fig. 3B). Each flagellum was roughly 5–7 lm long.

Transmission electron microscopy revealed that the cytoplasm contained a nucleus, mitochondria, Golgi bodies, amylopectin granules and electron-dense granules (Fig. 4A, B). The mitochondria were particularly prevalent around the periphery of the cell, while the amylopectin granules occurred throughout the cell body (Fig. 4). Longitudinal arrays of microtubules were seen subtending the plasma membrane in both the cross (Fig. 4C) and longitudinal sections (Fig. 4D, E). Surface folds were also present in both sections as protrusions of the plasma membrane and cytoplasm (Fig. 4C–E). A system of endomembrane vesicles was observed between the layer of pellicular microtubules and mitochondria (Fig. 4C–E).

The flagellar apparatus was located at the apical end of the cell and consisted of two flagella (anterior and posterior), two corresponding basal bodies, two anterior roots (ARa, b), one posterior root (PR) and a fibrous root connective (RC) that spanned between the ARb and PR (Figs 5, 6). The flagella themselves were comprised of nine doublets around

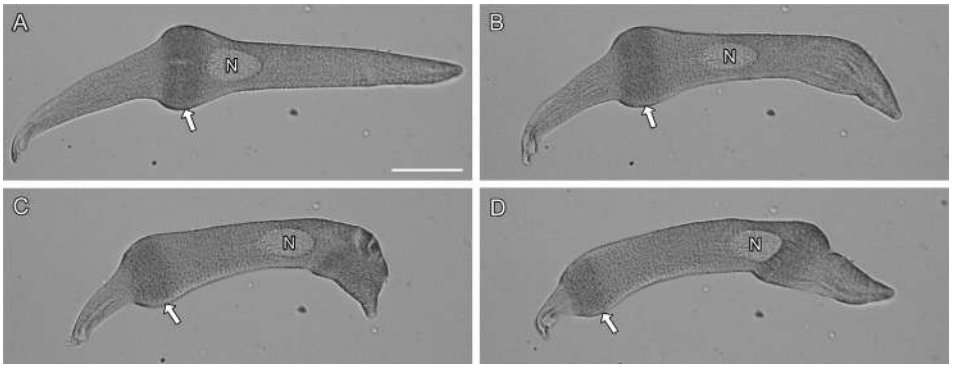

Figure 2. Light micrographs of *Platyproteum noduliferae* n. sp. showing peristalsis-like movement. Arrows indicate the waving cell from posterior to anterior. N, nucleus. Scale bars = 30 μm.

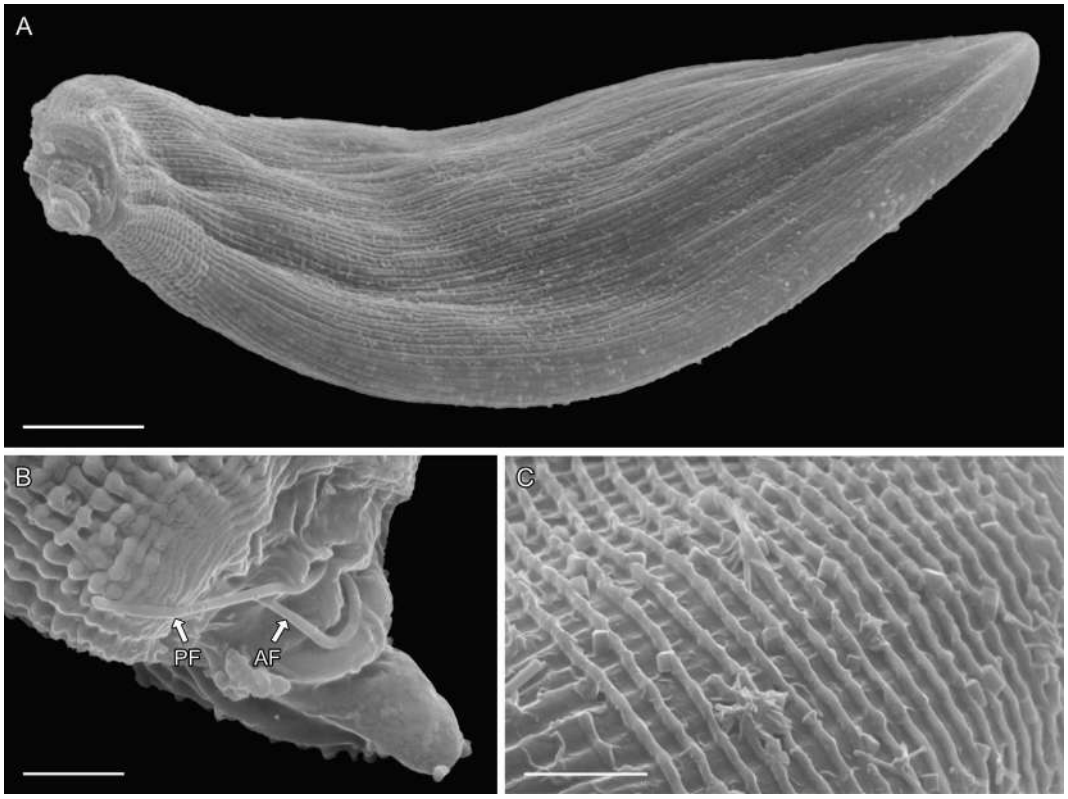

Figure 3. Scanning electron micrographs of *Platyproteum noduliferae* n. sp. (**A**) Whole cell. Mucron oriented to the left. Longitudinal surface folds run the entire length of the cell, and transverse surface folds are seen in the apical part of cell. (**B**) An enlarged image of the apical end of cell, showing anterior and posterior flagella (AF and PF, respectively) protruding from the base of mucron. (**C**) An enlarged image showing the longitudinal and transverse surface folds forming a criss-cross lattice. Scale bars: A = 20 μm; B, C = 3 μm.

a central pair (Fig. 5A). Each basal body and its transition zone were constituted in similar fashion with nine doublets, but the central pair was not observed (Fig. 5B, C); typical nine-triplet microtubules were not found. The two basal bodies were roughly parallel to each other and positioned about 1 lm apart. The flagella were inserted vertically into the cell, with little or no surrounding depression (i.e., no flagellar pocket). Each of the basal bodies were approximately 100 nm in length (Fig. 5D, E). The transitional plate is situated at the cell surface level, and the axosome lies just above this plate (Fig. 5D, E). Serial TEM cross-sections showed the anterior basal body attached to two flanking roots (ARa

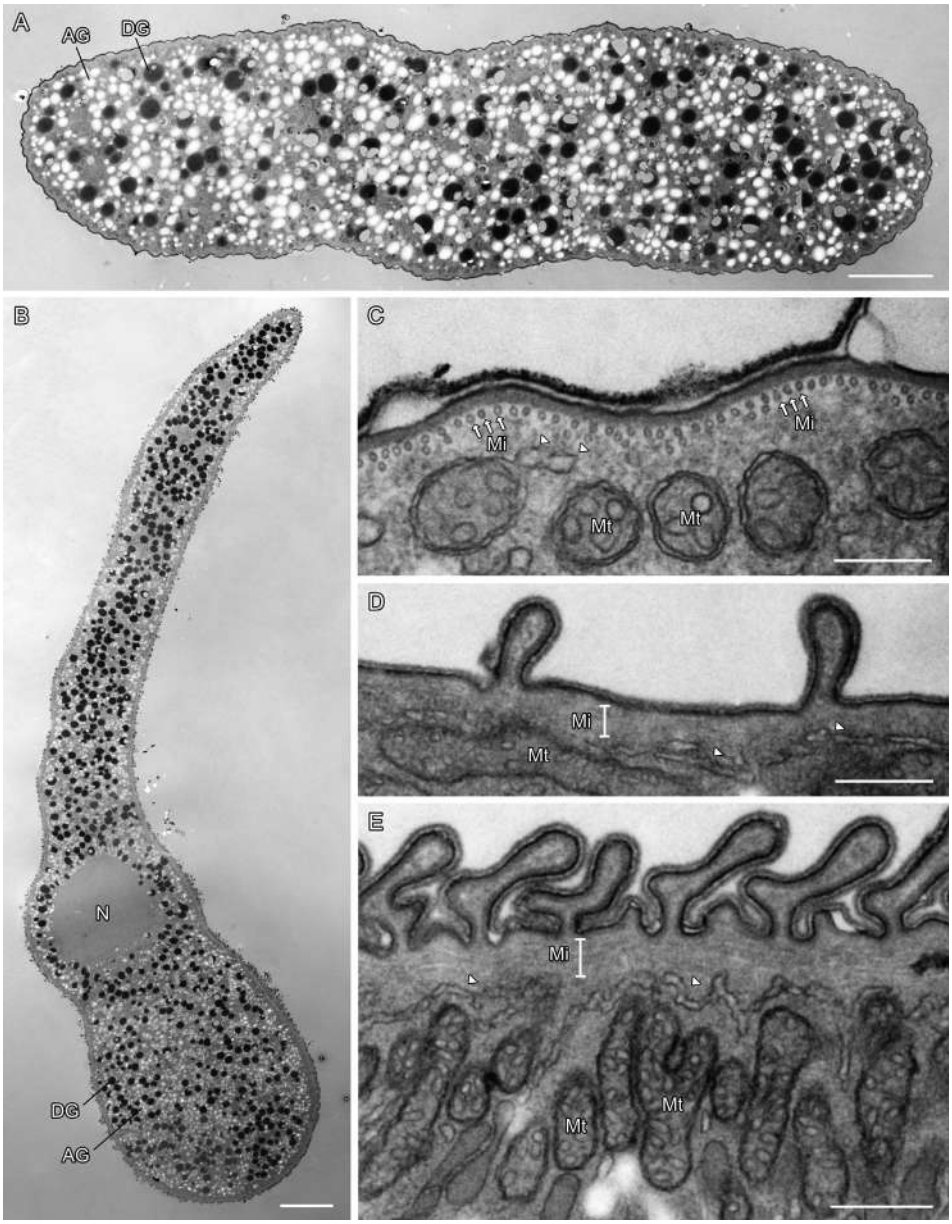

Figure 4. Transmission electron micrographs of *Platyproteum noduliferae* n. sp. showing general subcellular morphology. (**A**) Cross and (**B**) longitudinal sections showing a nucleus (N), amylopectin granules (AG), and dense granules (DG). (**C–E**) Peripheral view of (**C**) cross and (**D, E**) longitudinal sections showing the transverse surface folds, cortical microtubules (Mi), mitochondria (Mt) and a system of endomembrane vesicles (arrowheads). Scale bars; A = 5 μm; B =10 μm; C = 250 nm; D, E = 500 nm.

and b), and the posterior basal body associated with one root (PR) (Figs 5F–I, 6). The ARb and the PR were connected by the fibrous RC structure (Figs 5H, I, 6D, I, J). The ARa appeared to go deeper into the cell, whereas the ARb and the PR ran along the periphery of the cell (Figs 5F–I, 6). The ARa and b and the PR were made of three, four, and five microtubules, respectively (Figs 5G, 6J, L). The 3D structure of the flagellar apparatus of *Platyproteum noduliferae* n. sp. was compared to that of other myzozoans reported by previous studies (Fig. 7, see Discussion).

Phylogenetic Analysis

The 40-taxon alignment of concatenated 18S+ITS +28S rDNA sequences placed *Platyproteum noduliferae* n. sp. in a clade with apicomplexans

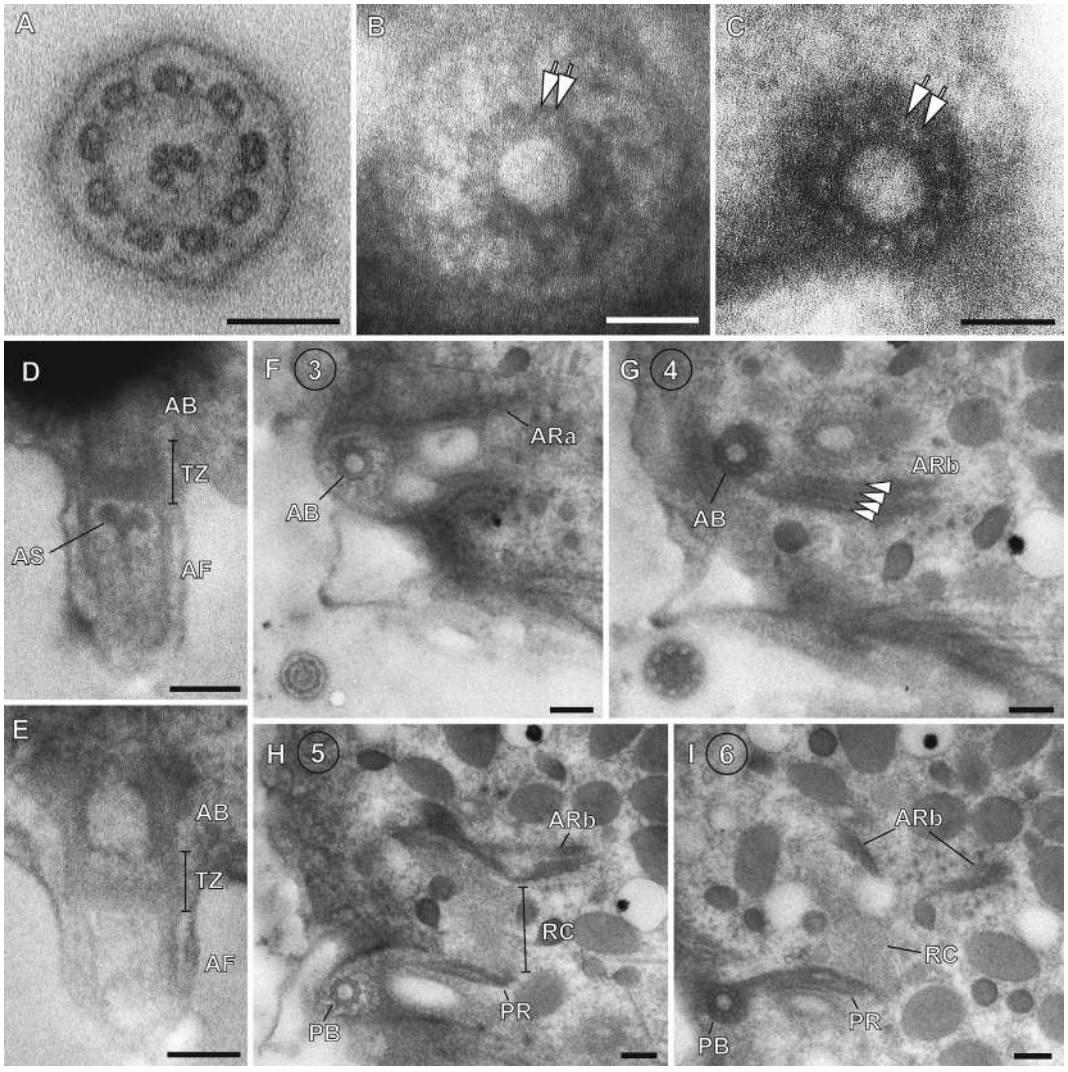

Figure 5. Transmission electron micrographs of *Platyproteum noduliferae* n. sp. flagella and flagellar apparatus in serial sections. Abbreviations: anterior basal body (AB); anterior flagellum (AF); anterior root a (ARa); anterior root b (ARb); axosome (AS); posterior basal body (PB); posterior root (PR); root connective material (RC); transition zone (TZ). (**A**) Cross section of a posterior flagellum comprised of nine sets of doublet microtubules and two central microtubules. (**B**) Cross section of a transition zone of a posterior flagellum. (**C**) A posterior basal body comprised of nine sets of doublet microtubules (arrows). (**D, E**) Longitudinal sections of an anterior basal body, an anterior flagellum with an axosome and their transition zone. (**F–**I) Serial sections of a same flagellar apparatus showing AB, ARa, ARb, PB, PR and RC. Four microtubules constituting ARb are seen (arrowheads). Section numbers are indicated in circles. Direction of sectioning is from the anterior to the posterior. Scale bars: A–E = 100 nm; F–I = 200 nm.

and chromerids (76 maximum likelihood bootstrap (BS), 0.98 Bayesian posterior probability (PP)) (Fig. 8A). *Platyproteum* was the deepest branch within this clade, but with negligible statistical support in the ML analysis (28 BS). The Bayesian tree showed a different topology (data not shown). The clade of dinoflagellates and perkinsids formed the sister group to the apicomplexans, chromerid and *Platyproteum* clade (Fig. 8A). The 43-taxon alignment of 18S rDNA sequences resulted in a robust clade of *P. noduliferae* n. sp. and *P. vivax* (100 BS, 1.00 PP), forming a clade with *Filipodium phascolosomae* and *Digyalum oweni* (48 BS, 0.96 PP) at the base of the apicomplexan and chromerid clade with low support (17 BS, 0.63 PP) (Fig. 8B; Supplementary Material Fig. S1), although the topology of chromerids slightly differed from the tree of 18S +ITS+28S rDNA sequences. The pairwise distance

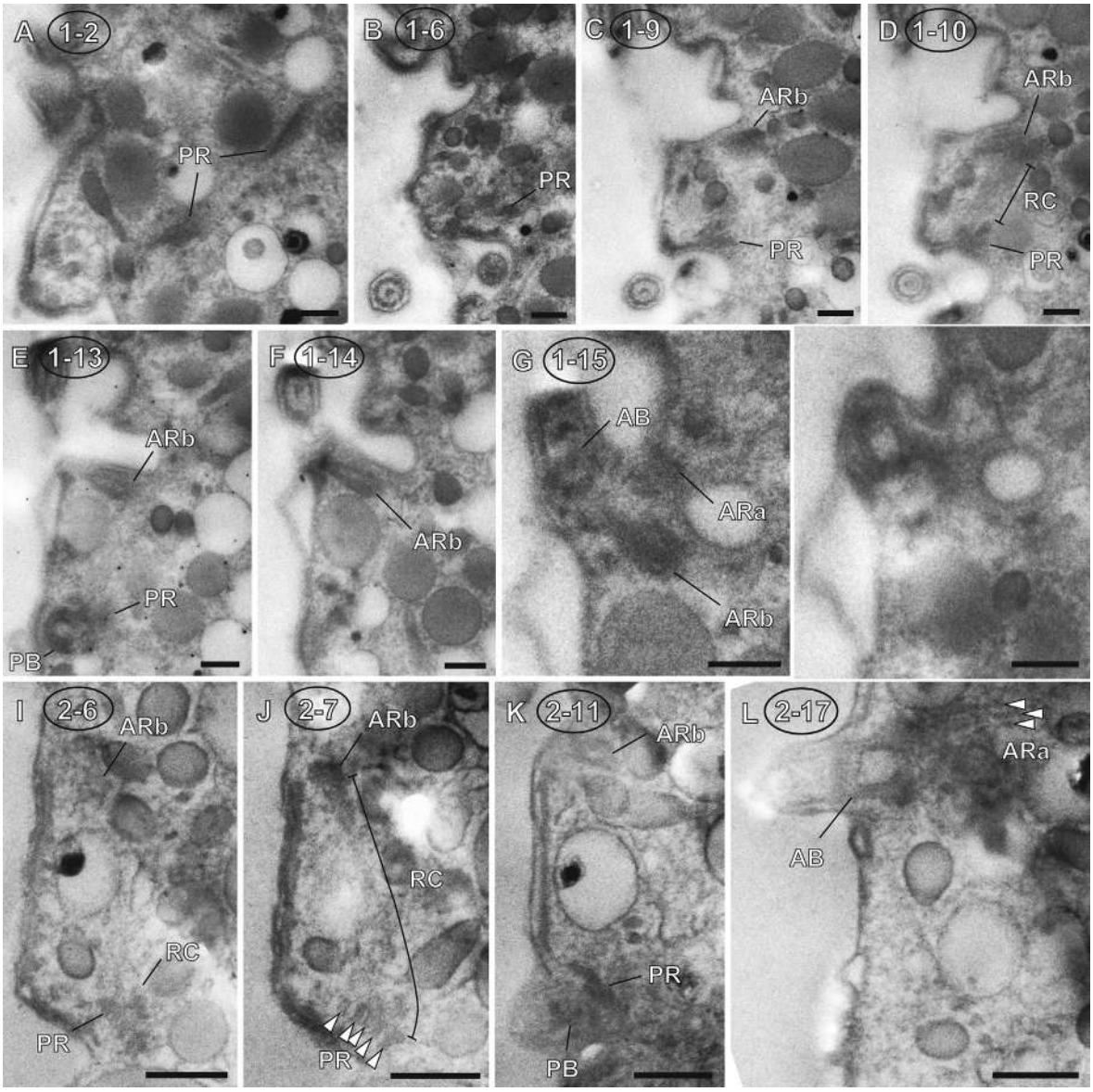

Figure 6. Transmission electron micrographs of *Platyproteum noduliferae* n. sp. flagella and flagellar apparatus in serial sections. Abbreviations: anterior basal body (AB); anterior root a (ARa); anterior root b (ARb); posterior basal body (PB); posterior root (PR); root connective material (RC). (**A–H**) and (**I–L**) show serial sections of the same flagellar apparatuses, respectively. Five microtubules constituting PR (J) and three microtubules constituting ARa (L) are seen (arrowheads). Directions of sectioning are from ventral to dorsal (A–H) and from left to right (I–L). Scale bars = 200 nm.

of 18S rDNA sequences of *P. noduliferae* n. sp. and *P. vivax* (1717 bps) was 23.1%.

Discussion

A New Species of *Platyproteum*

Platyproteum noduliferae n. sp. possesses morphological and behavioral characteristics that are similar to *P. vivax*. These similarities include the overall flattened shape, the extreme contortions of the cell body in live specimens, and the presence of transverse surface folds, which are all consistent with diagnostic traits that were suggested when this genus was introduced (Leander, 2006; Rueckert and Leander, 2009). On the other hand, the size of the trophozoit stage differed between these two species. *Platyproteum noduliferae* n. sp. was observed to reach approximately 120 lm when fully

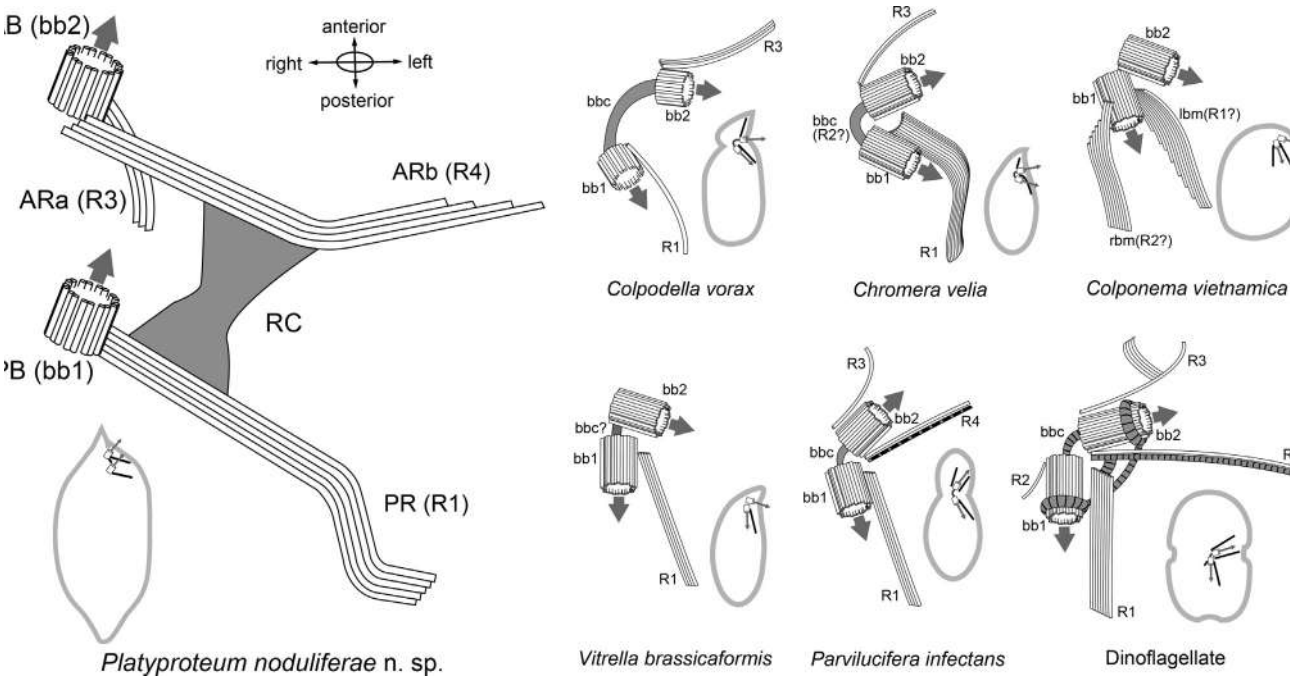

Figure 7. Schematic reconstructions of the flagellar apparatuses of *Platyproteum noduliferae* n. sp. and six other alveolates: *Colpodella vorax* (Brugerolle, 2002; Okamoto and Keeling, 2014), *Chromera velia* (Moore et al., 2008; Portman et al., 2014), *Vitrella brassicaformis* (Füssy et al., 2017; Oborník et al., 2012), *Parvilucifera infectans* (Norén et al., 1999; Okamoto and Keeling, 2014), a typical dinoflagellate (Moestrup, 2000; Okamoto and Keeling, 2014) and *Colponema vietnamica* (Tikhonenkov et al., 2014). Abbreviations: anterior basal body (AB); anterior root a and 2 (ARa and 2); basal body 1 and 2 (bb1 and 2); basal body connective (bbc); left bands of microtubules (lbm); posterior basal body (PB); posterior root (PR); root 1 to 4 (R1 to 4); right bands of microtubules (rbm); root connective (RC).

stretched, whereas *P. vivax* has been observed around 550 lm (Gunderson and Small, 1986), 150 to 425 lm (Leander and Keeling, 2003) and 120 to 500 lm (Leander, 2006). In addition, although both species parasitize sipunculid hosts, the host for *P. noduliferae* n. sp. is *Phascolosoma noduliferum* whereas the host for *P. vivax* is *Phascolosoma agassizii*. There is also a difference in the appearance of longitudinal surface folds. Leander (2006) reported that *Selenidium vivax* (= *P. vivax*) has longitudinal striations, but the protrusion of the plasma membrane is modest compared to the striations of *P. noduliferae* n. sp. Moreover, the transverse folds of *P. vivax* contain tiny longitudinal ridges (Leander 2006), whereas those of *P. noduliferae* n. sp. is mixed with complete longitudinal folds, which form a criss-cross lattice.

The molecular phylogenetic analyses recovered *Platyproteum noduliferae* n. sp. as a sister species to *P. vivax*. The phylogenetic trees suggest that *P. noduliferae* n. sp. and *P. vivax* branch at the base of the chrompodellids and apicomplexans together with *Filipodium phascolosomae* and *Digyalum oweni*, although statistical support is low. This tree topology is consistent with the contemporary understanding of *Platyproteum* phylogenetics provided by Mathur et al. (2019). In their phylogenomic analysis of an unidentified *Platyproteum* species, they also showed that the genus falls outside of Apicomplexa altogether, instead forming a distinct lineage at the base of apicomplexans and chrompodellids. *Platyproteum, Selenidium and Filipodium* can commonly often be found co-infecting the same sipunculid individual (Rueckert and Leander, 2009; Wakeman, 2020). It is evident that sipunculids have been infected independently by myzozoans more than once. This hints at the possibility of many more myzozoan and apicomplexan parasites yet to be discovered from sipunculids. To this end, this multi-parasite system in sipunculids might also be an intriguing model to further study the interactions (or niche partitioning) among parasites harbored by a single host.

The presence of transverse striations, the distinct contortions of the cell body, and the overall tape-like, flattened morphology adhere to the diagnostic

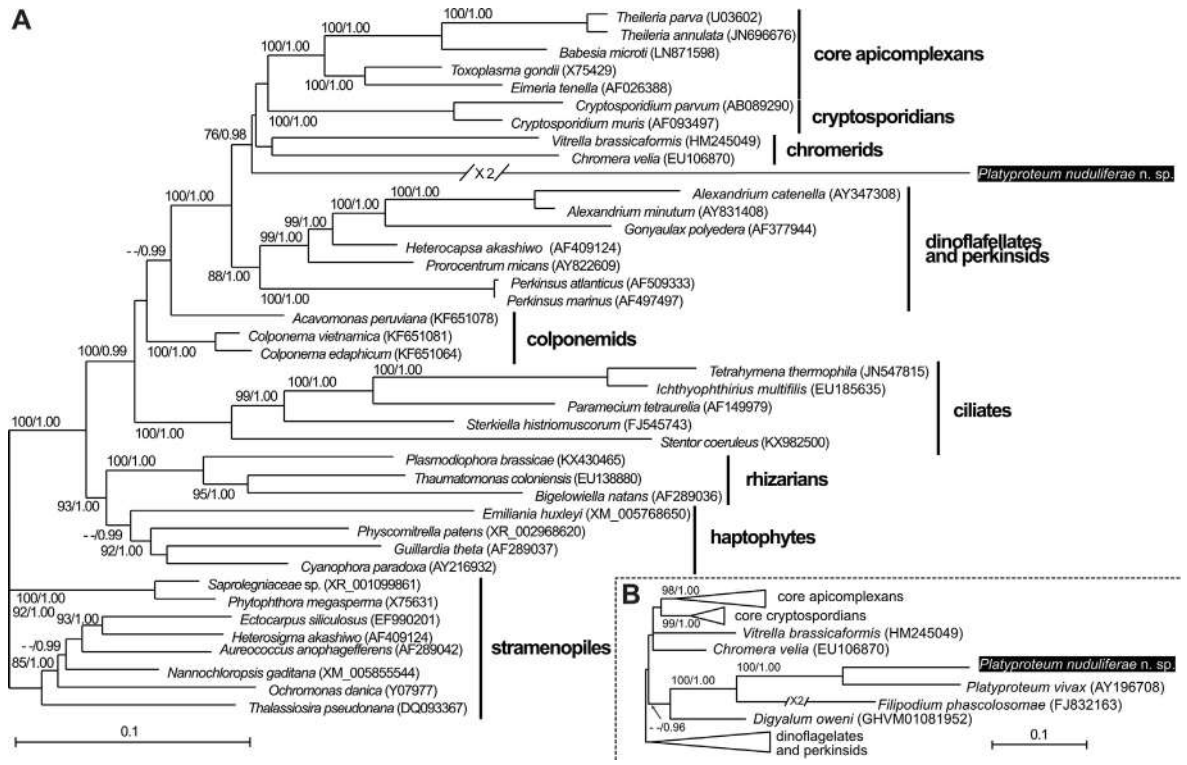

Figure 8. (**A**) Maximum likelihood tree of concatenated 18S + ITS + 28S rDNA sequence. (**B**) Maximum likelihood tree of 18S rDNA sequences. White triangles are collapsed taxa. Numbers indicate maximum likelihood bootstrap percentages, followed by Bayesian posterior probabilities. Bootstrap support /posterior probability below 70/0.95 are not displayed. Sequences from this study are highlighted with a black box.

traits of *Platyproteum*, distinguishing this lineage from related taxa: *Filipodium* and *Digyalum* (Table 1). Taking into consideration the morphological and behavioral characteristics of *Platyproteum noduliferae* n. sp., the diagnostic criteria for *Platyproteum*, and the divergence between the rDNA sequences of *P. vivax*, *P. noduliferae* n. sp. represents a distinct, previously undescribed species. The continued discovery and characterization of additional myzozoan taxa, especially from sipunculids, is key to further constructing a taxonomic framework that accurately reflects the phylogeny of taxa that diverged near the base of apicomplexans and chrompodellids.

Flagellar Apparatus

Our study demonstrated the presence of the flagella and flagellar roots in a member of *Platyproteum* for the first time. Leander (2006) mentions apical pores, "threadshaped structures" protruding from these pores, and an "unidentified linear structure" in *P. vivax*, but did not identify these as a flagellar apparatus. With the benefit of our data from *P. noduliferae* n. sp., we can identify these "thread-like" and "linear" structures in *P. vivax* as flagella and part of one of the microtubular roots (ARb or PR), respectively. It is possible that these structures were too small to be recognized as flagella and roots in the previous studies.

Considering the positions of flagella in the cell of *Platyproteum noduliferae* n. sp. and the convention suggested by Moestrup (2000), the posterior flagellum likely corresponds to the number 1 flagellum and the anterior flagellum corresponds to the number 2 flagellum (Fig. 7). The posterior root and the anterior roots a and b would be interpreted as root 1, 3, and 4, respectively (Moestrup, 2000). Compared to flagellar apparatuses of other myzozoanorganisms such as chrompodellids (Brugerolle, 2002; Foissner and Foissner, 1984; Füssy et al., 2017; Moore et al., 2008; Oborník et al., 2012; Okamoto and Keeling, 2014; Portman et al., 2014), *P. noduliferae* n. sp. is unique in its possession of both the roots 3 and 4, unlike studied chrompodellids which lack at least one of these. Thus, roots 3 and 4 are thought to be less conserved within myzozoan-related lineages. The repertoire of roots

Table 1. Morphological comparison of *Platyproteum noduliferae* n. sp. and relevant organisms. Created based upon Table 1 from Rueckert and Leander (2009).

	Platyproteum noduliferae n. sp.	*Platyproteum vivax* (typespecies)	*Selenidium pendula* (typespecies)	*Selenidium orientale*	*Selenidium pisinnus* sp.	*Filipodium phascolosomae*	*Filipodium ozakii* (typespecies)	*Filipodium aspidosiphoni*	*Digyalum oweni* (tyoespecies)
Host	*Phascolosoma noduliferum*	*Phascolosoma agassizii*	*Nerine cirratulus*	*Themiste pyroides*	*Phascolosoma agassizii*	*Phascolosoma agassizii*	*Siphonosoma cumanense*	*Aspidosiphonclavatus*	*Littorina* species
Host tissue	Intestine	Intestine	Intestine	Intestine	Intestine	Intestine	Intestine	Intestine	Intestine
Locality	W. Pacific	E. Pacific	E. Atlantic	E. and W. Pacific	E. Pacific	E. Pacific	W. Pacific	Mediterranean	E. and W. Atlantic
Trophozoites									
Shape	Tape-like	Tape-like	Spindle-shaped	Spindle-shaped, flattened	Oblong to elliptoid	Triangular to elliptoid	Cylindrical and flattened	Triangular	Pear-shaped
Size (L × W, μm)	111–121 × 29–43	120–500 × 15–80	180 × 30–40	64–100 × 9–25	120–300 × 15–41	85–142 × 40–72	350 × 30–105	60	25 × 15
Nucleus									
Shape	Oval	Round to oval	Round to oval	Ellipsoidal	Ellipsoidal	Spherical	Lens-shaped	Oval	Round
Size (L × W or Ø, μm)	16–17 × 10–13	7–36	18–33 × 13–32	8–15 × 10–25	5 × 11	20–30			
Position	Posterior to the transverse midline	Middle	Middle	Middle	Anterior half	Anterior	Middle	Anterior	Middle
Mobility	Folding, twisting, peristalsis	Folding, twisting, peristalsis	Bending, twisting, pendulum-like	Bending, twisting, pendulum-like	Bending, twisting, pendulum-like	Bending, twisting, stretching	Bending	“amoeboid”	
Longitudinal surface folds	Yes	No	Yes	Yes	Yes	Unknown	Yes	Unknown	No
Total number	Many		20–30	18–20	40–44		Many		
Transverse surface folds	Yes	Yes	Unknown	No	No	Unknown	No	Unknown	Yes
Hair-like projections	No	No	No	No	No	Yes	Yes (retractable?)	Yes	No
Shape of mucron	Hook-like	Edge-like	Pointed	Pointed	Pointed	Edge-like	Edge-like	Edge-like	Pointed
Literature	This study	Gunderson and Small (1986); Leander (2006)	Levine (1971); Schrével (1970)	Simdyanov and Kuvardina (2007); Rueckert and Leander (2009)	Rueckert and Leander (2009)	Rueckert and Leander (2009)	Hoshide and Todd (1992, 1996); Hukui (1939)	Tuzet and Ormières (1965)	Dyson et al. (1993); Janouškovec et al. (2019)

in *P. noduliferae* n. sp. resembles that of dinoflagellates (although root 2 has been reported from some dinoflagellates including perkinsids), but the components of the roots are different. In the case of *P. noduliferae* n. sp., roots 3 and 4 consist of multiple microtubules, rather than a single microtubule, and root 4 lacks the transverse striated root (TSR) (Moestrup, 2000; Norén et al., 1999; Okamoto and Keeling, 2014). The current information suggests that the single microtubule in root 3 and the TSR in root 4 have likely been acquired by dinoflagellates after the divergence of the other myzozoan lineages. *Colponema vietnamica* Tikhonenkov, Mylnikov and Keeling, 2013, which is a member of a group that diverged earlier from myzozoans, has been reported to possess two bands of microtubules at left and right side of the posterior flagellum (lbm and rbm)(Tikhonenkov et al., 2014). These likely corresponding to roots 1 and 2, respectively, while any structure corresponding to roots 3 and 4 cannot be recognized. Tikhonenkov et al. (2014) also reported the presence of secondary microtubules (sm) from the band of microtubules (bm) near the proximal end of the kinetosome of the flagellum, although it is unclear whether these structures correspond to any kind of roots. Root 1, consisting of multiple microtubules, seems to be conservative within the myzozoans and *Colponema*, and root 2 seems to have been reduced within the myzozoans after the divergence of *Colponema*.

Each flagellum of *Platyproteum noduliferae* n. sp. was comprised of typical nine doublets + central pair microtubules. On the other hand, each basal body was revealed to be comprised of nine doublets of microtubules, in contrast to most other eukaryotes with basal bodies comprised of nine triplets. This nine-doublet structure of the basal body has also been described in *Colpodella vorax* (Kent 1880) Simpson & Patterson, 1996, which is presumably a member of chrompodellids (Brugerolle, 2002); although its phylogeny has not been revealed due to a lack of molecular data. The basal bodies of *P. noduliferae* n. sp. are also similar in their short length (100 nm) to those found in *C. vorax* (150 nm). However, such traits of basal bodies are not shared among chrompodellids; for example, *Vitrella brassicaformis* Oborník & Lukeš, 2012 possesses approximately 200 nm–long basal bodies comprised of nine triplets (Füssy et al., 2017). *Chromera velia* Moore et al., 2008 also has long (approximately 500 nm) basal bodies (Moore et al., 2008; Oborník et al., 2011), although the number of microtubules comprising the basal bodies has not been reported.

In addition, the basal bodies of *Platyproteum noduliferae* n. sp. are also distinctive in being separated from each other and not joined directly by any connective material. Many myzozoans have basal bodies that are linked by a basal body connective (bbc) (Okamoto and Keeling, 2014; Yubuki et al., 2016). Although a bbc was not reported for *Vitrella brassicaformis*, a structure resembling a bbc is visible (Füssy et al. 2017; see Fig. 1B, therein). The basal bodies of some *Colpodella* species are similar to that of *P. noduliferae* n. sp. in that they are distant from each other, but they are interconnected with connective material (Brugerolle, 2002; Okamoto and Keeling, 2014). In the case of *P. noduliferae* n. sp., the basal bodies are associated indirectly via a posterior root, anterior root b and a root connective. Although the root connective is similar to the striated root connective (SRC) that links roots 1 and 4 in many dinoflagellates (Okamoto and Keeling, 2014), it is unclear whether they are homologous, considering the phylogenetic relationships and the absence of SRC in other relatives.

The basal bodies in *Platyproteum noduliferae* n. sp. and *Colpodella vorax* are relatively similar based on the nine-doublet microtubules, their short length and their distant location. It is noteworthy that *P. noduliferae* n. sp. and *Colpodella* spp. are heterotrophic organisms, unlike their phototrophic relatives, namely *Vitrella brassicaformis* and *Chromera velia* (Brugerolle, 2002; Moore et al., 2008; Oborník et al., 2012). Moreover, apicomplexans are composed of obligate parasitic organisms and lack basal bodies and flagella throughout much of their life cycle. The transition from autotrophy to heterotrophy/parasitism might have caused such structural changes or significant reduction of the basal bodies. However, the available information is not enough to discuss the character evolution of the flagellar apparatus across all myzozoan-related organisms. Especially, *Colpodella* species whose flagellar apparatuses have been surveyed, but remains an enigma because they have not been investigated by large scale molecular phylogenetic approaches. Further information on the ultrastructure and phylogenetic relationships would improve

our understanding of the evolution within these parasitic myzozoans.

Taxonomic Summary

Platyproteum noduliferae n. sp. Yokouchi, Iritani, Lim, Phua, Horiguchi and Wakeman, 2021

Description Trophozoite is elongate and flat with length and width of 111 to 121 lm and 29 to 43 lm, respectively, while in its leaf-like shape. Nucleus is oval with a major axis of 16 to 17 lm and a minor axis of 10 to 13 lm. Mucron at apical end of trophozoite is hook-like. Two flagella protrude from base of mucron. Longitudinal and transverse surface folds line the surface of whole and apical part of trophozoite, respectively. Movement by stretching, contacting and peristalsis.

Type locality Oshoro, Hokkaido, Japan (43° 12055.200N 140°51017.200E)

Type host *Phascolosoma noduliferum* Stimpson, 1855 (Sipuncula, Phascolosomatidea, Phascolosomatida, Phascolosomatidae)

Location in host Intestinal lumen

Hapantotype Trophozoites on SEM stubs with a gold sputter coat have been stored in the algal and protist collection in the Hokkaido University Museum (KCW_platy_2021); all individuals were taken from the same host.

Iconotype Fig. 1A; this individual was taken from the same host as the hapantotype.

Gene Sequence A partial sequence covering a large portion of the ribosomal operon (18S rRNA–28S rRNA genes) has been deposited in GenBank: LC663666; genetic sequences came from individuals isolated from the same host.

Etymology The species name, *noduliferae*, refers to the host species, *Phascolosoma noduliferum*, from which the species was isolated.

Methods

Host collection and parasite isolation: *Phascolosoma noduliferum* Stimpson 1855 was collected from Oshoro, Hokkaido, Japan (43°12055.200N 140°51017.200E) during the summer of 2019, and again in April and May 2021. Animals were found inhabiting the spaces between the roots of seagrass. The worms were transported back to the laboratory and dissected within 48 hours of collection. The procedure involved carefully extracting the digestive tract from the base of the proboscis to the anus. The entire digestive tract was split down its length using fine forceps to expose the contents of the gut in filtered seawater (0.45 lm). Parasites were observed under an inverted light microscope and isolated using hand-drawn glass pipettes. Individual parasites from each host were then washed multiple times in filtered seawater (0.45 lm) and pooled together for subsequent use in light microscopy or scanning electron microscopy. Single-cell isolations were prepared for DNA extraction and sequencing.

Light microscopy, scanning electron microscopy and transmission electron microscopy: Light micrograph images and videos were taken using a Zeiss Axioscope (Carl-Zeiss, Göttingen, Germany) inverted microscope connected to a Canon EOS Kiss X9i camera (Tokyo, Japan). For scanning electron microscopy, individuals were transferred to a 3–5 lm mesh filter in 2.5% glutaraldehyde in seawater by micropipette and held on ice for 15 min. After washing the samples three times (5 min each) in seawater, 1% OsO_4 in water was placed on the samples for 30 min. The samples were subsequently washed with distilled water and dehydrated through a graded series of ethanol mixtures (30%, 50%, 75%, 80%, and 3x 100%) for 5 min at each step. Samples were critical point dried with CO_2, sputter-coated with 5 nm gold and viewed using a Hitachi N-3000 (Tokyo, Japan) SEM. For transmission electron microscopy, individual cells were fixed in 2.5% glutaraldehyde in seawater on ice for 30 min, washed in seawater, and post fixed with 1% OsO_4 in water on ice for 1.5 hours; both fixation steps were performed in the dark. Following the fixation with OsO_4, samples were washed in seawater, and dehydrated through a graded series of ethanol mixtures (30%, 50%, 75%, 80%, and 3x 100%) for 5 min at each step, and subsequently moved to a 1:1 acetone/ethanol mixture, and a 100% acetone solution for 10 min each. Samples were then placed in a 1:1 resin (Agar Low Viscosity Resin, Agar Scientific, Essex, UK)/acetone mixture for 30 min, followed by 100% resin overnight at room temperature. Resin was exchanged the following day, and samples were polymerized at 68°C for 32 hours. Samples were cut with a diamond knife into 70 nm thick sections and viewed with a Hitachi-7400 (Tokyo, Japan) TEM.

DNA extraction, PCR amplification, and sequencing: Single-cell isolates of each parasite were placed in 0.2 ml PCR tubes. Total genomic DNA was extracted using a FFPE DNA extraction kit (Lucigen, Wisconsin, USA) following the manufacturers protocol. The primer pairs SR1 and D1R_specR, Gen18S_1700F and RB, D1RF1 and Gen3000R were initially used to amplify the total 18S, 28S rDNA and internal transcribed spacer (ITS) region using the following protocol on a thermal cycler: Initial denaturation 95 °C 5:00 min; 35 cycles of 95 °C 0:30 s, 52 °C 0:30 s, 72 °C 3:30 min; final extension 72 °C 7:00 min. Subsequently, 1ll of the initial PCR relation was used in a second PCR with following primer pairs SR1 and SR5TAK, SR1 and SR9, SR8TAK and D1R_specR, Gen18_1700F and D1R_specR, D1RF1 and D2C, D1R_conF and RB, D3A and Gen2500R, D3A and RB, Gen2000F and Gen2500R, V2000F and RB, Gen2200F and RB, Mid_conF and Gen_2500R, Mid_conF and RB, End_conF and Gen3000R under the following parameters: Initial denaturation 95 °C 5:00 min; 25 cycles of 95 °C 0:30 s, 52 °C 0:30 s, 72 °C 2:00 min; final extension 72 °C 7:00 min. In each PCR reaction, TaKaRa Ex Taq (Takara Bio Inc., Otsu, Japan) was used, following the manufacturer's protocols. PCR products were purified using a Qiagen PCR purification kit (Qiagen, Germantown, USA); 1 μl of purified product was used in a sequencing reaction with ABI BigDye Terminator v3.1 (Applied Biosystems, Massachusetts, USA) and subsequently purified with ethanol, before being eluted in 18 μl Hi-Di Formamide (Applied Biosystems, Massachusetts, USA) and sequenced on a 3130 Genetic Analyzer (Applied Biosystems, Massachusetts, USA). All primers used in this study are listed in Supplementary Material Table S1.

Phylogenetic analyses: New sequences generated in this study were identified by BLAST. Two molecular phylogenetic datasets were generated and viewed using Mesquite 3.6 (Maddison and Maddison, 2015): 1) a concatenated 18S+ITS+28S rDNA alignment (40 taxa) and 2) an 18S rDNA alignment (43 taxa) including three related species, *Platyproteum vivax*, *Filipodium phascolosomae* and *Digyalum oweni*. MUSCLE (Edgar, 2004) was used under the

default settings to align all datasets used for phylogenetic analyses. The alignment was trimmed with Gblocks (Castresana, 2000; Talavera and Castresana, 2007), only selecting for allowing gaps within the final blocks then checked with Mesquite. Final alignments used for phylogenetic analyses included 1474 and 4301 bp for 18S rDNA and the concatenated 18S+ITS+28S rDNA datasets, respectively.

The best-fit model for each dataset was selected using IQ-TREE under AICc (Trifinopoulos et al., 2016). Maximum-likelihood analyses, including non-parametric bootstrapping, on the two datasets were subsequently run with IQ-TREE using TIM3+F+R4 and TIM2+F+R5, as the model of evolution for the 18S rDNA and the concatenated 18S+ITS+28S rDNA datasets, respectively. Each analysis ran for 1000 bootstrap pseudoreplicates.

All Bayesian analyses were performed using the program MrBayes 3.2.5 (Ronquist and Huelsenbeck, 2003). The program was set to operate with GTR+I+G, and four Monte Carlo Markov Chains (MCMC) starting from a random tree. A maximum of 50,000,000 runs were performed for 18S and concatenated 18S+ITS+28S rDNA datasets. Generations were calculated with trees sampled every 100 generations and the first 25% of trees in each run were discarded as burn-in. The program was terminated at 500,000 runs when the standard deviation of split frequencies fell below 0.01. Convergence was confirmed in Tracer 1.7 (Rambaut et al., 2018). Posterior probabilities correspond to the frequency at which a given node was found in the post-burn-in trees.

ZooBank registration: The electronic edition of this article conforms to the requirements of the amended International Code of Zoological Nomenclature, and hence the new names contained herein are available under that Code from the electronic edition of this article. This published work and the nomenclatural acts it contains have been registered in ZooBank, the online registration system for the ICZN. The ZooBank LSIDs (Life Science Identifiers) can be resolved and the associated information viewed through any standard web browser by appending the LSID to the prefix http://zoobank.org/. The LSID for this publication is: urn:lsid:zoobank.org:pub:C25A1ACC-2919-4363-BF1B-2B9D2BC5A7D7. The electronic edition of this work was published in a journal with an ISSN.

Conflict of Interest

The authors declare that there is no existing conflict of interest for this manuscript, or the data within.

Acknowledgements

This work was supported by Japanese Society for the Promotion of Science (JSPS) grants 18K14774 and PG6R180004 to KCW. Doctoral grants through JSPS (JP19J20893) and MEXT supported KY and DI, respectively. A Japanese Science Society (JSS) Sasagawa 2018-5037 was also provided to (DI). Samples were collected with the support of Oshoro Marine Station. Support for the critical point drying of samples was provided by the Research Faculty of Agriculture at Hokkaido University.

Appendix A. Supplementary Data

Supplementary data to this article can be found online at https://doi.org/10.1016/j.protis.2022.125878.

References

Adl SM, Bass D, Lane CE, Lukeš J, Schoch CL, Smirnov A, Agatha S, Berney C, Brown MW, Burki F, Cárdenas P, Čepička I, Chistyakova L, del Campo J, Dunthorn M, Edvardsen B, Eglit Y, Guillou L, Hampl V, Heiss AA, Hoppenrath M, James TY, Karnkowska A, Karpov S, Kim E, Kolisko M, Kudryavtsev A, Lahr DJ, Lara E, Le Gall L, Lynn DH, Mann DG, Massana R, Mitchell EA, Morrow C, Park JS, Pawlowski JW, Powell MJ, Richter DJ, Rueckert S, Shadwick L, Shimano S, Spiegel FW, Torruella G, Youssef N, Zlatogursky V, Zhang Q (2019) Revisions to the classification, nomenclature, and diversity of eukaryotes. J Eukaryot Microbiol **66**:4–119

Brugerolle G (2002) *Colpodella vorax*: ultrastructure, predation, life-cycle, mitosis, and phylogenetic relationships. Europ J Protistol **38**:112–125

Castresana J (2000) Selection of conserved blocks from multiple alignments for their use in phylogenetic analysis. Mol Biol Evol **17**:540–552

Cavalier-Smith T (2004) Only six kingdoms of life. Proc Roy Soc B-Biol Sci **271**:1251–1262

Cavalier-Smith T, Chao EE (2004) Protalveolate phylogeny and systematics and the origins of Sporozoa and dinoflagellates (phylum Myzozoa nom. nov.). Europ J Protistol **40**:185–212

Edgar RC (2004) MUSCLE: multiple sequence alignment with high accuracy and high throughput. Nucleic Acids Res **35**:1792–1797

Foissner W, Foissner I (1984) First record of an ectoparasitic flagellate on ciliates: An ultrastructural investigation of the morphology and the mode of attachment of *Spiromonas gonderi* nov. spec. (Zoomastigophora, Spiromonadidae) invading the pellicle of ciliates of the genus Colpoda (Ciliophora, Colpodidae). Protistologica **20**:635–648

Francia ME, Striepen B (2014) Cell division in apicomplexan parasites. Nat Rev Microbiol **12**:125–136

Füssy Z, Masařová P, Kručinská J, Esson HJ, Oborník M (2017) Budding of the alveolate alga *Vitrella brassicaformis* resembles sexual and asexual processes in apicomplexan parasites. Protist **168**:80–91

Gunderson J, Small EB (1986) *Selenidium vivax* n. sp. (Protozoa, Apicomplexa) from the sipunculid *Phascolosoma agassizii* Keferstein, 1867. J Parasitol **72**:107–110

Hoppenrath M (2017) Dinoflagellate taxonomy — a review and proposal of a revised classification. Mar Biodiv **47**:381–403

Hoshide K, Todd KS (1992) Structure and function of the mucron of *Filipodium ozakii* Hukui, 1939, (Apicomplexa, Gregarina). Proc Zool Soc (Calcutta) **45**:53–59

Hoshide K, Todd KS (1996) The fine structure of cell surface and hair-like projections of *Filipodium ozakii* Hukui 1939 gamonts. Acta Protozool **35**:309–315

Hukui T (1939) On the gregarines from *Siphonosoma cumanense* (Keferstein). J Sci Hiroshima Univ **7**:1–23

Janouškovec J, Tikhonenkov DV, Burki F, Howe AT, Kolísko M, Mylnikov AP, Keeling PJ (2015) Factors mediating plastid dependency and the origins of parasitism in apicomplexans and their close relatives. Proc Natl Acad Sci USA **112**:10200–10207

Janouškovec J, Gavelis GS, Burki F, Dinh D, Bachvaroff TR, Gornik SG, Bright KJ, Imanian B, Strom SL, Delwiche CF, Waller RF, Fensome RA, Leander BS, Rohwer FL, Saldarriaga JF (2017) Major transitions in dinoflagellate evolution unveiled by phylotranscriptomics. Proc Natl Acad Sci USA **114**:E171–E180

Kuvardina ON, Leander BS, Aleshin VV, Myl'nikov AP, Keeling PJ, Simdyanov TG (2002) The phylogeny of colpodellids (Alveolata) using small subunit rRNA gene sequences suggests they are the free-living sister group to apicomplexans. J Eukaryot Microbiol **49**:498–504

Leander BS (2006) Ultrastructure of the archigregarine *Selenidium vivax* (Apicomplexa) – a dynamic parasite of sipunculid worms (host: *Phascolosoma agassizii*). Mar Biol Res **2**:178–190

Leander BS (2008) Marine gregarines: evolutionary prelude to the apicomplexan radiation? Trends Parasitol **24**:60–67

Leander BS, Keeling PJ (2003) Morphostasis in alveolate evolution. Trends Ecol Evol **18**:395–402

Levine ND (1971) Taxonomy of Archigregarinorida and Selenidiidae (Protozoa, Apicomplexa). J Protozool **18**:704–717

Maddison WP, Maddison DR (2015) Version 3.04 Mesquite: a modular system for evolutionary analysis Version 3.04. http://mesquiteproject.org

Mathur V, Kolísko M, Hehenberger E, Irwin NA, Leander BS, Kristmundsson Á, Freeman MA, Keeling PJ (2019) Multiple independent origins of apicomplexan-like parasites. Curr Biol **29**, 2936.e5–2941.e5

Moestrup Ø (2000) The flagellate cytoskeleton: introduction of a general terminology for microtubular flagellar roots in protists. In Leadbeater BSC, Green JC (eds) The Flagellates: Unity, Diversity and Evolution. Taylor & Francis; London, p. 67–94

Moore RB, Oborník M, Janouškovec J, Chrudimský T, Vancová M, Green DH, Wright SW, Davies NW, Bolch CJ, Heimann K, Šlapeta J, Hoegh-Guldberg O, Logsdon JM, Carter DA (2008) A photosynthetic alveolate closely related to apicomplexan parasites. Nature **451**:959–963

Morrison DA (2009) Evolution of the Apicomplexa: where are we now? Trends Parasitol **25**:375–382

Norén F, Moestrup Ø, Rehnstam-Holm AS (1999) *Parvilucifera infectans* Noren et Moestrup gen. et sp. nov. (Perkinsozoa phylum nov.): A parasitic flagellate capable of killing toxic microalgae. Europ J Protistol **35**:233–254

Oborník M, Vancová M, Lai DH, Janouškovec J, Keeling PJ, Lukeš J (2011) Morphology and ultrastructure of multiple life cycle stages of the photosynthetic relative of apicomplexa, *Chromera velia*. Protist **162**:115–130

Oborník M, Modrý D, Lukeš M, Černotíková-Stříbrná E, Cihlář J, Tesařová M, Kotabová E, Vancová M, Prášil O, Lukeš J (2012) Morphology, ultrastructure and life cycle of *Vitrella brassicaformis* n. sp., n. gen., a novel chromerid from the Great Barrier Reef. Protist **163**:306–323

Okamoto N, Keeling PJ (2014) The 3D structure of the apical complex and association with the flagellar apparatus revealed by serial TEM tomography in *Psammosa pacifica*, a distant relative of the apicomplexa. PLoS One **9**:e84653

Portman N, Foster C, Walker G, Šlapeta J (2014) Evidence of intraflagellar transport and apical complex formation in a free-living relative of the apicomplexa. Eukaryot Cell **13**:10–20

Rambaut A, Drummond AJ, Xie D, Baele G, Suchard MA (2018) Posterior summarization in Bayesian phylogenetics using Tracer 1.7. Syst Biol **67**:901–904

Ronquist F, Huelsenbeck JP (2003) MrBayes 3: bayesian phylogenetic inference under mixed models. Bioinformatics **19**:1572–1574

Rueckert S, Leander BS (2009) Molecular phylogeny and surface morphology of marine archigregarines (Apicomplexa), *Selenidium* spp., *Filipodium phascolosomae* n. sp., and *Platyproteum* n. g. and comb. from North-Eastern Pacific peanut worms (Sipuncula). J Eukaryot Microbiol **56**:428–439

Schrével J (1970) Contribution a l'étude des Selenidiidae parasites d'annélides polychètes. I. Cycles biologiques. Protistologica **6**:389–426

Simdyanov TG, Kuvardina ON (2007) Fine structure and putative feeding mechanism of the archigregarine *Selenidium orientale* (Apicomplexa: Gregarinomorpha). Europ J Protistol **43**:17–25

Simpson AG, Patterson DJ (1996) Ultrastructure and identification of the predatory flagellate *Colpodella pugnax* Cienkowski (Apicomplexa) with a description of *Colpodella turpis* n. sp. and a review of the genus. Syst Parasitol **33**:187–198

Talavera G, Castresana J (2007) Improvement of phylogenies after removing divergent and ambiguously aligned blocks from protein sequence alignments. Syst Biol **56**:564–577

Tikhonenkov DV, Janouškovec J, Mylnikov AP, Mikhailov KV, Simdyanov TG, Aleoshin VV, Keeling PJ (2014) Description of *Colponema vietnamica* sp.n. and *Acavomonas peruviana* n. gen. n. sp., two new alveolate phyla (Colponemidia nom. nov. and Acavomonidia nom.nov.) and their contributions to reconstructing the ancestral state of alveolates and eukaryotes. PLoS One **9**:e95467

Trifinopoulos J, Nguyen LT, von Haeseler A, Minh BQ (2016) W-IQ-TREE: a fast online phylogenetic tool for maximum likelihood analysis. Nucleic Acids Res **44**: W232–W235

Tuzet O, Ormières R (1965) Sur quelques grégarines parasites de *Phascolion* et *Aspidosiphon* (Sipunculiens). Protistologica **1**:43–48

Wakeman KC (2020) Molecular phylogeny of marine gregarines (apicomplexa) from the Sea of Japan and the northwest Pacific including the description of three novel species of Selenidium and Trollidium akkeshiense n. gen. n. sp. Protist **171**:125710

Yubuki N, Čepička I, Leander BS (2016) Evolution of the microtubular cytoskeleton (flagellar apparatus) in parasitic protists. Mol Biochem Parasitol **209**:1–2

Available online at: www.sciencedirect.com

ScienceDirect

View publication stats